Exoplanetary transits in the Galactic bulge

Statistical study of near-IR variability in VVV Survey M dwarf stars

Thiago Ferreira dos Santos & **Roberto Kalbusch Saito** Contact: t.ferreira@astro.ufsc.br

Universidade Federal de Santa Catarina, Brazil

The photometric and astrometric selection of M dwarf stars

Making use of VVV Survey (Minniti et al. 2010) multicolour data for tile b294, located towards the Milky Way bulge ($1.5° \times 1°$ centered at l, $b = 3.88°, -3.14°$), we selected M dwarf stars in order to analyse photometric variations due to exoplanets-like objects orbiting such stars. Several effects increase the likelihood of life on M dwarf planets, including their abundance in the Galaxy (≈85% of 100+ billion stars) and the intense cloud formation on the star-facing side of tidally locked planets, responsible to reduce the overall thermal flux and equilibrium temperature differences between two sides of a planet (Yang et al. 2013).

Both giant and red dwarf stars of spectral subtype M present similar near-IR colours range, for instance in (J−H) and (H−Ks) colours, which makes the photometric selection solely inefficient. We adopted $\mathrm{H}_J > 68.9(\mathrm{J-Ks}) - 50.7$ for M dwarf stars in order to perform a better distinction between such objects making use of the astrometric data from the VVV InfraRed Astrometric Catalogue (VIRAC, Smith et al. 2018), calculating the reduced proper motion of selected objects according to eq. (1). Moreover, from the Gaia DR2 data (Gaia Collaboration et al. 2018), we selected only stars with parallax measurements larger than $\varpi = 1$ *mas*, especially due to the relative proximity of M dwarf stars in the magnitude range of our data, which consequently present high proper motion, in contrast to red giant stars, further away however reddish due to extinction effects in the Milky Way.

$$\mathrm{H}_J = J + 5\log_{10}(\mu) = J + 5\log_{10}\left(\sqrt{\mu^2_{\alpha\cos\delta} + \mu^2_\delta}\right) \tag{1}$$

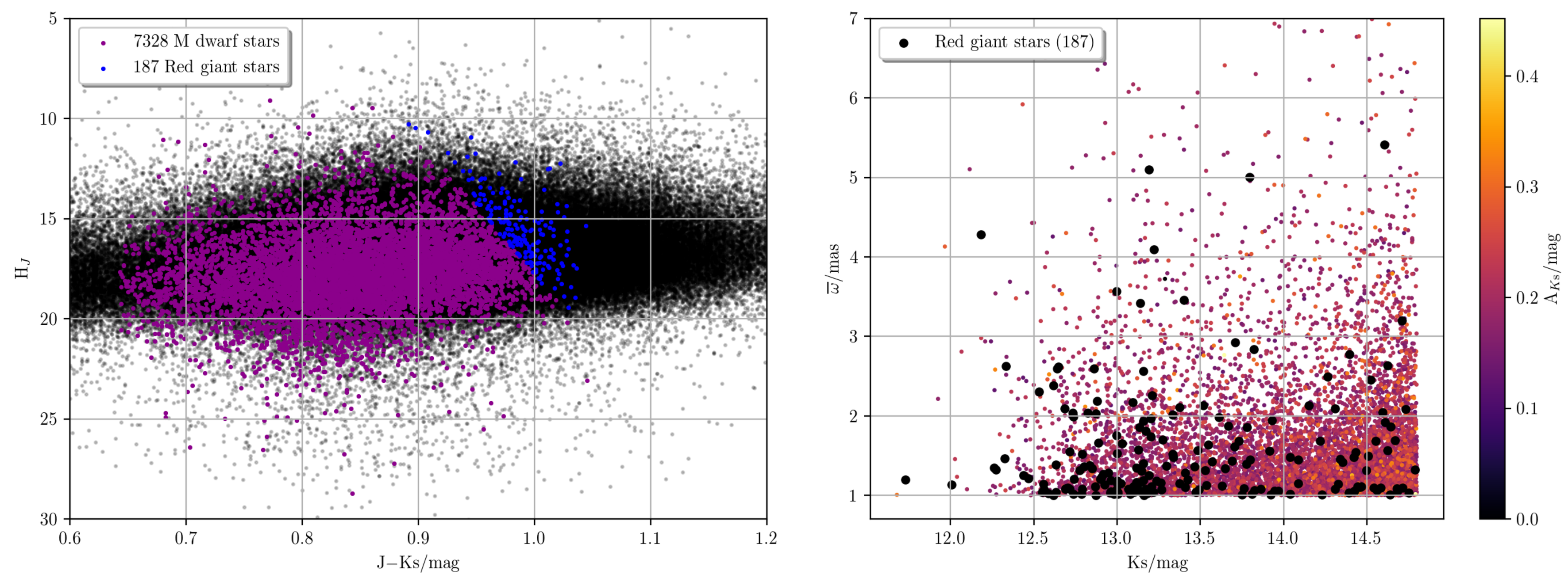

Figure 1: *Left:* Relationship between J−Ks colour and the reduced proper motion for stars with Ks-mag $< 14.8^m$. Purple dots represent M dwarf stars and blue dots red giant stars spurious to our current analysis. *Right:* Relationship between parallax and Ks-mag for selected stars. Black dots represent red giant stars and the colour-index the extinction levels in Ks filter.

Photometric variations in exoplanet-M dwarf system are relatively small, typically about 0.15^m in Ks filter (λ_{Ks} = 2.14 nm), therefore we arbitrarily limited our selection in the VVV Ks-band PSF light-curves to Ks $< 14.8^m$, consequently $\sigma_{Ks} < 0.05^m$, which is expected to reduce the incidence of false positives in our analysis. Furthermore, based on their near-IR colours, we estimated the spectral subtype for M dwarf class as function of the colours $\Gamma \equiv$ Y−J, $\Pi \equiv$ Y−Ks and $\Upsilon \equiv$ H−Ks, following eq. (2), also estimated the distance of such objects making use of the observational apparent and theoretical magnitudes in J filter (λ_J = 1.25 nm; Rojas−Ayala et al. 2014) according to $d \equiv m_J - M_J = 5\log d - 5$.

$$\{\mathbf{MX}(\Gamma,\Pi,\Upsilon)\}^{9}_{\mathbf{X}=0} = 5.394(\Gamma) + 4.370(\Gamma)^2 + 24.325(\Pi) - 7.614(\Pi)^2 + 7.063(\Upsilon) - 20.779 \tag{2}$$

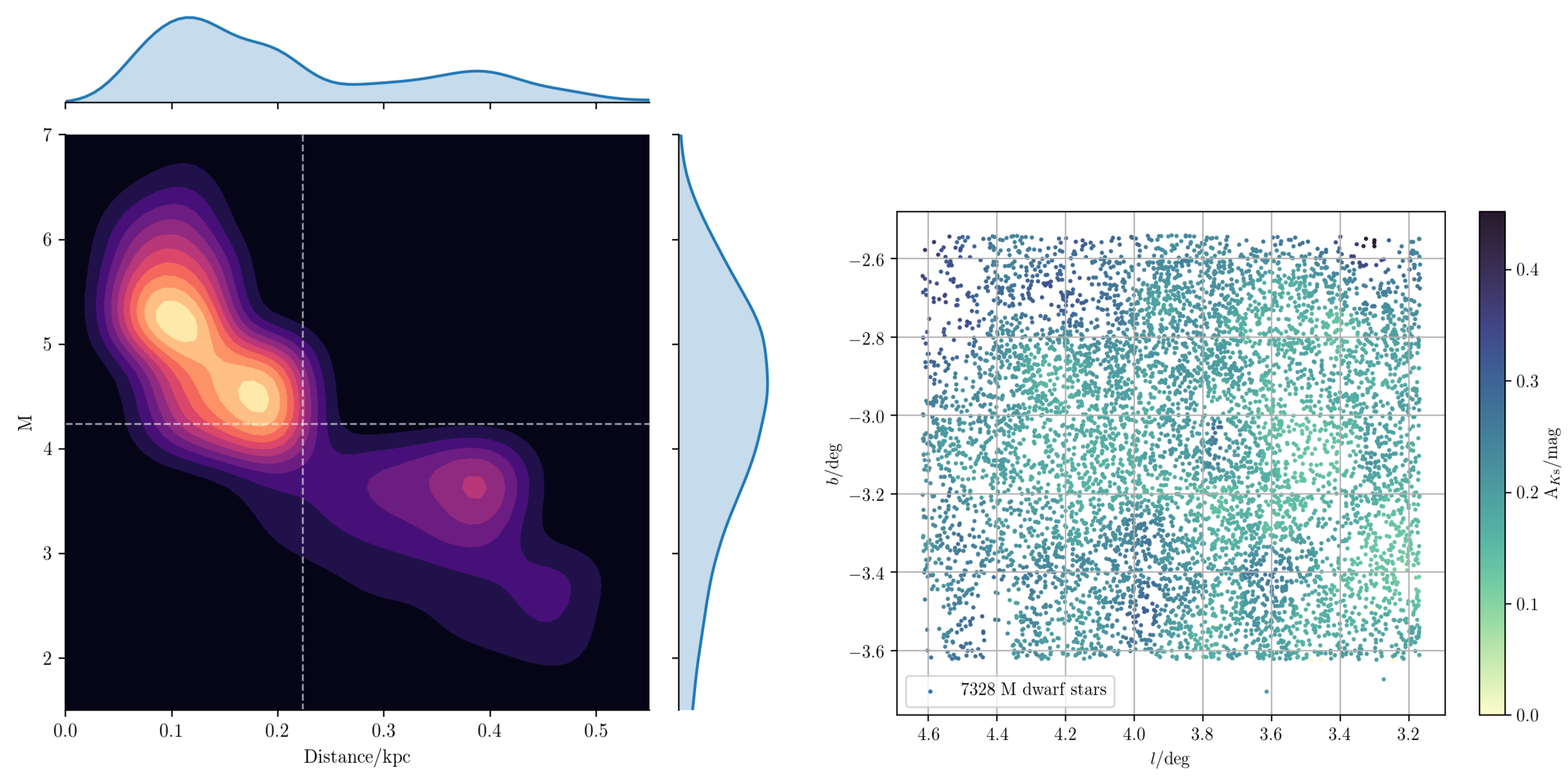

Figure 2: *Left:* Spectral subtype and distance relationship for M dwarf stars selected. *Right:* Location in Galactic coordinates of such stars, with colours indicating the extinction in Ks filter toward the region observed.

It is not surprising to say that one of the main objective of exoplanetary studies nowadays are focused on the detection and subsequent characterisation of potentially habitable water-supported rocky exoplanets, in other words, objects orbiting the so-called habitable zone (HZ) of its central star (Kopparapu et al. 2013). Exoplanets with masses up to ≈ 0.10 M⊕ represent a potential study laboratory for the origin of organic life, however, the detection of minerals only found in meteorites, such as $(Fe,Cr)_{1.15}(Ti,Fe)_2S_4$ (Heideite), $Na_2Mg_4Cr_2^{3+}(Si_6O_{18})O_2$ (Krinovite) and $Fe^{0+}_{1.5}Ni_{0.5}P$ (Barringerite) for instance, may indicate numerous different chemical compositions in exoplanetary systems, preventing in a certain level environments conducive to the presence and maintenance of organic life (Gaidos & Selsis 2007).

The Box-fitting least-squares (BLS) method

In opposition to commonly implemented Fourier-like sinusoidal methods, the BLS is a stat method developed by Kóvacs et al. (2002) in order to detect transit-like candidates by potenti oplanets (even exoplanetary systems and/or exomoons) modelling a periodic upside-down bo time-series photometric data-set $\Lambda \doteq \{t_k, y_k|\sigma_k\}, k = 1, 2, ..., n$. Four main parameters derived the Python implementation ASTROPY used in this work are the orbital period (P_{orb}), transit du (τ), transit depth (δ) and a reference mid-transit time by the first event (φ). The algorithm as follow: *i)* select a period and event duration grids that best apply to the case of M dwar orbited by exoplanets; *ii)* apply a *sigma-clip* $\sigma = 3$ cut in Λ, which removes some outliers; *iii)* a minimisation of $\mathcal{O}(i_1, i_2)$, function of the ingress and egress times, which determines the wid also the position of the *box* on a phase diagram.

Following the definition, $\mathcal{L} \triangleq \Delta\mathrm{K_s} = \max(\delta) \equiv \mathcal{H} - \mathcal{L}$ and $\mathcal{H} \triangleq \Delta\mathrm{K_s} \approx 0$, the different $\partial_{(\mathcal{L},\mathcal{H})}\mathcal{O}(i_1, i_2) = 0$, yields to the minimisation of the residual sum of squares.

$$\mathcal{O}(i_1, i_2) = \sum_{i=1}^{i_1-1}\tilde{\omega}_i^2(\tilde{x}_i - \mathcal{H})^2 + \sum_{i=i_1}^{i_2}\tilde{\omega}_i^2(\tilde{x}_i - \mathcal{L})^2 + \sum_{i=i_2+1}^{n}\tilde{\omega}_i^2(\tilde{x}_i - \mathcal{H})^2$$

$$\tilde{x}_i = \begin{cases}\mathcal{L}, & \text{if } i \in [i_1, i_2]\\ \mathcal{H}, & \text{if } i \in [1, i_1) \cup (i_2, n]\end{cases}$$

Furthermore, the maximisation of $\mathcal{O}(i_1, i_2)$ yields to an (i_1,i_2)-independent equation, with $\sum_{i_1}^{i_2}\tilde{\omega}_i^2$ and $\gamma \equiv \sum_{i_1}^{i_2}\tilde{\omega}_i^2\tilde{x}_i$, where we can re-write the equation (3) following:

$$\mathcal{O} = \sum_{i=1}^{n}\tilde{\omega}_i^2\tilde{x}_i^2 - \frac{\gamma^2}{\beta - \beta^2}$$

It is remarkable to note that the third term of equation (5) is (i_1,i_2)-independent, so we can the Signal-Residue (III) following equation (6), which can be used to characterise the qualit the significance of the signal found.

$$\mathrm{III} = \max\left[\sqrt{\frac{\gamma^2}{\beta - \beta^2}}\right]$$

Some preliminary results

From the 4.592.102 sources presented in the b294 tile catalogue, 7238 M dwarf stars were se after the photometric and astrometric processes previously described, which about 350 of the senting possible exoplanetary transits such as those presented in Fig. 3.

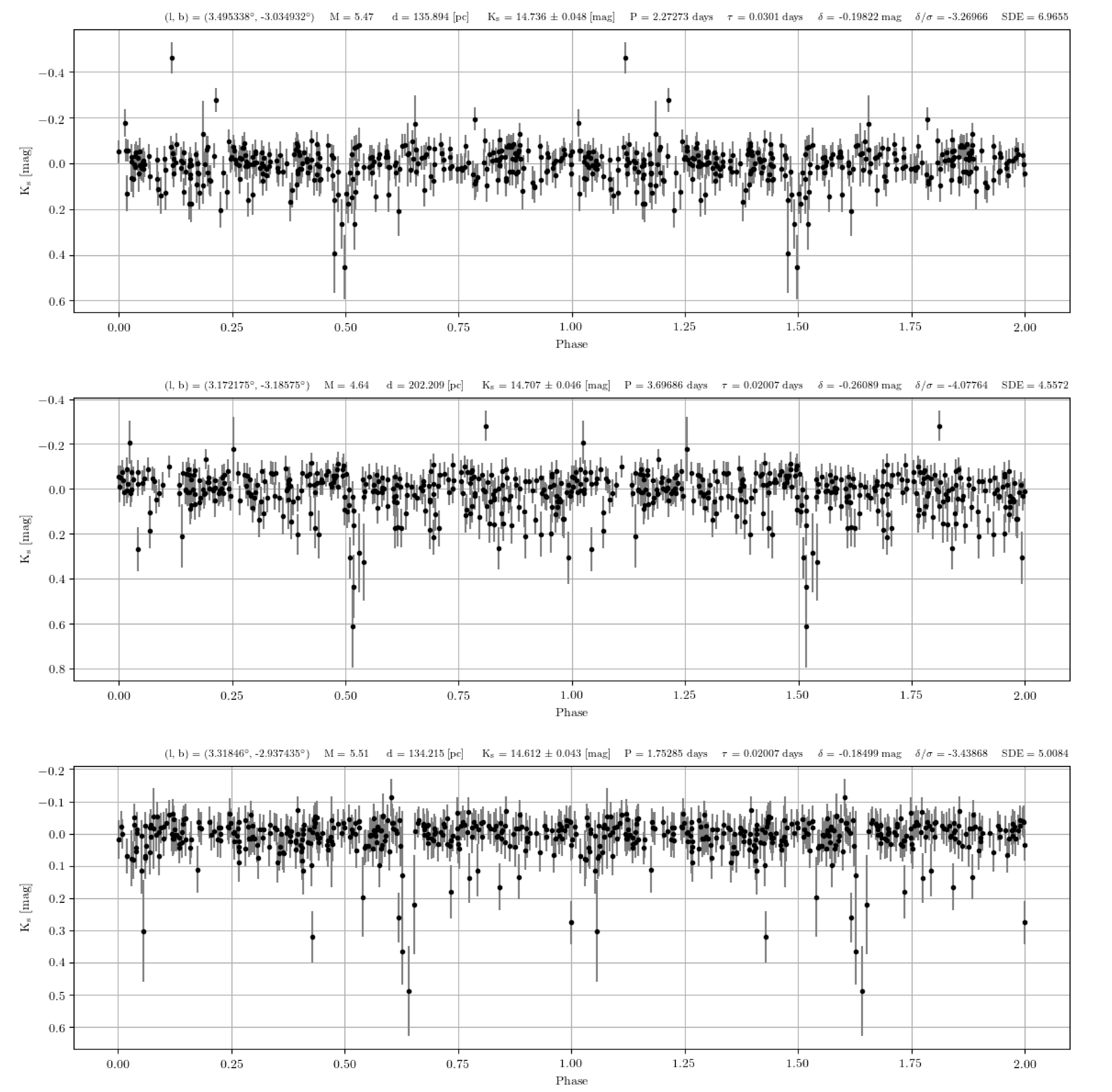

Figure 3: Phase diagrams for selected objects, with *Phase* following the definition $\varphi = mod(\Lambda_{t_k}, P_{orb}) \in [0, 1]$. The main param exoplanetary transits events are presented in the top-right corner of each panel.

Bibliography

Gaia Collaboration, et al., 2018, A&A, 616, A1.
Gaidos, E. & Selsis, F., 2007, *Protostars and Planets V*, P929.
Kopparapu, R. K., et al., 2013, ApJ, 765 .
Kovács, G., et al., 2002, AA, 391, 369.
Minniti, D., et al., 2010, NewA, 15, 433-443.
Rojas-Ayala, B., et al., 2014, A&A, 571, A36.
Smith L. C., et al., 2018, MNRAS, 474, 1826.
Yang, J., et al., 2013, ApJ, 771.

We gratefully acknowledge use of data from the ESO Public Survey programme ID 179.B-2002 taken with the VISTA telescope, products from the Cambridge Astronomical Survey Unit (CASU). Thiago Ferreira acknowledge support from PIBIC@UFSC and CNP